

Analysis of Ultra-fast Kelvin Waves Simulated by the Kyushu University GCM

Ying-Wen Chen and Saburo Miyahara

Department of Earth and Planetary Sciences, Kyushu University, Japan

1. Introduction

Equatorial Kelvin waves are one of important global scale motions that only propagate toward eastward and are trapped in the equatorial region. This kind of waves was first theoretically found by Matsuno (1966) and many observational facts show that this kind of waves exists in the atmosphere.

Observational facts show that prominent periods of equatorial Kelvin waves vary with height in the atmosphere. Hirota (1977) found using metrological rocket observational data that the prominent period of equatorial Kelvin waves in the upper stratosphere is about 10 days with zonal wavenumber 1 ($s=1$) components which are called as fast Kelvin waves. Salby (1983) indicated that equatorial Kelvin waves whose periods are in the period band of about 3-6 days with $s=1$ components can be found in the lower mesosphere and these waves are called ultra-fast Kelvin waves. Ultra-fast Kelvin waves are also found in the mesosphere and lower thermosphere region by radar observations (Riggin et al., 1997; Pancheva et al., 2004). Pancheva et al. (2004) also especially indicated that the vertical wavelength of the zonal wind field of 3-day ultra-fast Kelvin waves in the lower thermosphere is about 49 km.

In this study, we focus on behaviors and vertical structures of ultra-fast Kelvin waves in the Kyushu University General Circulation Model (the Kyushu GCM) in the winter time. Horizontal and vertical structures of ultra-fast Kelvin waves in this model will be figure out.

2. Data

Data used in this study are data simulated by the Kyushu GCM T42L250 version (Yoshikawa and Miyahara, 2005). The coverage of this model is from the surface to 150 km height with 250 layers. The vertical resolution of this model in the stratosphere, mesosphere, and lower thermosphere is about 500 m and the horizontal resolution of this model is triangular-truncation at wavenumber 42. Physical processes that are thought to be excitation sources of ultra-fast Kelvin waves in the tropical troposphere regions such as moist convective heating (e.g. Forbes, 2000; Mayr et al., 2004) are included in this model.

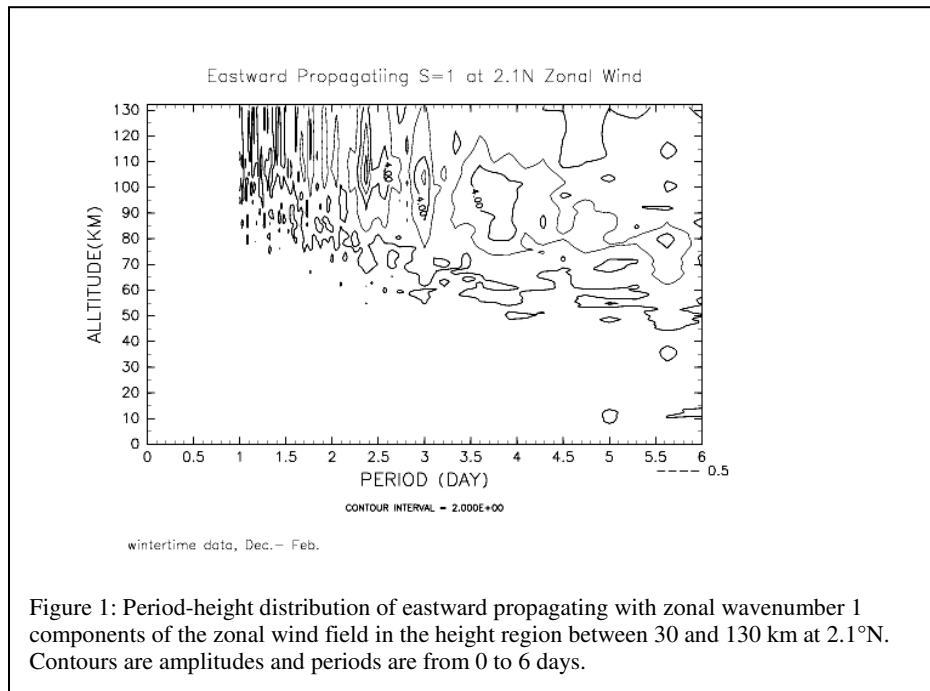
In this study, the bi-hourly sample dataset of winter time including December, January and February are used. Data of the zonal wind, meridional wind, and the

geopotential height fields are mainly analyzed.

3. Results

3.1 Period-height Distribution

Eastward propagating with $s=1$ components are extracted out by applying space-time Fourier analysis on the three-month data, as shown in figure 1. As can be seen in figure 1, at 2.1°N , there are some prominent peaks appearing in the height region above about 70 km in the period between 2 and 4 days. In present study, we focus on the structures and vertical propagation of 3-day eastward propagating with $s=1$ components to figure out behaviors of this kind of waves.



3.2 3-Day Period $S=1$ Structure

The horizontal sections of eastward propagating 3-day period with $s=1$ components of the wind and geopotential height fields in the height region of 80-130km are shown in figure 2. As shown in this figure, the wind and geopotential height fields have structures of Kelvin waves in this height region, especially in the height region between 80 and 100 km. As it can be seen, structures of waves are symmetric about the equator in the height region between 80 and 100 km while the symmetric axis of this kind of waves shifts a little beat to the north (at 110 km) and south (at 120 km). Although the symmetric axis shifts in this high region, it can still be identified that westerlies correspond with positive deviation of the geopotential height field and easterlies correspond with negative deviation of the geopotential height regions.

Structures of Kelvin waves of 3-day period with $s=1$ components are confirmed in the height region of 80-130 km. Amplitudes of the geopotential height field of this kind of waves are mainly confined in the region between about 40°N and 40°S .

Vertical sections of the zonal wind and geopotential height fields averaged over 10.5°N to 10.5°S are shown in figure 3. As shown in this figure, phase lines of the zonal wind and geopotential height fields mainly tilt toward east with height. Phase lines of the geopotential height field tilt toward east continuous from the height about 30 km, while that of the zonal wind field tilt toward east clearly from the height about 80 km. This may be caused by the reason that the zonal wind field is contaminated easily by noise than the geopotential height field. The average vertical wavelength of this kind of waves is about 50 km which can be estimated from both the zonal wind and geopotential height fields.

Figure 4 shows the Hough function of eastward propagating 3-day period with $s=1$ mode. In this case, the equivalent depth is 2241 m and the vertical wavelength is about 52 km for a 256 K isothermal atmosphere. It shows that the amplitude of this kind of waves is trapped in the region between about 40°N and 40°S and the maximum of the amplitude of this kind of waves appears at the equator. Comparing this result with the analysis result shown in figure 1, maxima of amplitudes of 3-day eastward propagating $s=1$ components appear around the equator and they are trapped in the region between about 40°N and 40°S , which is consistent with the Hough function shown in figure 4. The averaged vertical wavelength estimated from vertical section as shown in figure 3 is about 50 km which is also consistent with the theoretical vertical wavelength 52 km.

The vertical profile of amplitude of the geopotential height fields averaged over 10.5°N to 10.5°S in the height region from 0 km to 130 km is shown in figure 5. As shown in this figure, the amplitude of the geopotential height field grows by a factor of nearly equal to $\exp(z/2H)$ rate with height in the region between 20 km and 100 km. This shows that this kind of waves propagates vertically with nearly conserving energy in the height region between 20 km and 100 km. The effect of viscosity is getting more significant in the region above about 100 km and this effect causes wave energy dissipation, so that amplitudes of the geopotential height fields can not continuously grow in the region above 100 km.

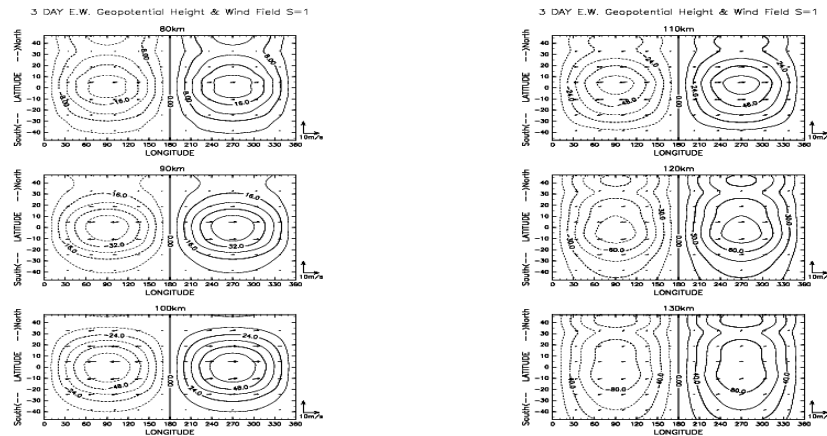


Figure 2: Horizontal sections of the wind (arrows) and geopotential height (contours) fields of 3-day eastward propagating with $s=1$ components from 80 km to 130 km. Latitudes are from 47.5°S to 47.5°N .

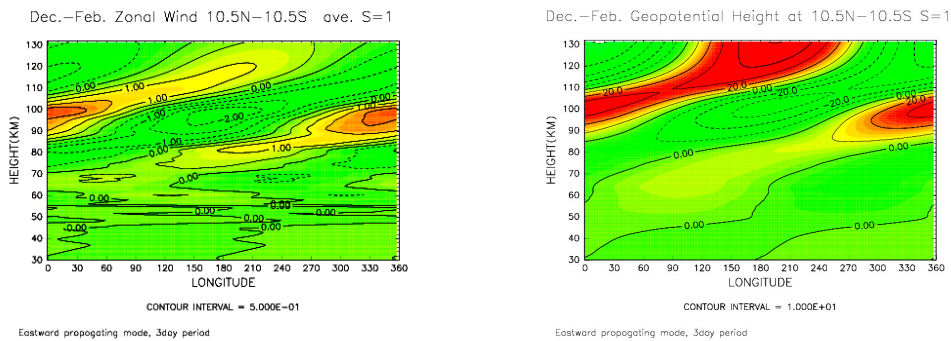


Figure 3: Vertical sections of 3 day eastward propagating with zonal wavenumber 1 components of the zonal wind (left) and geopotential height (right) fields averaged over 10.5°N to 10.5°S . Height region is from 30 km to 130 km.

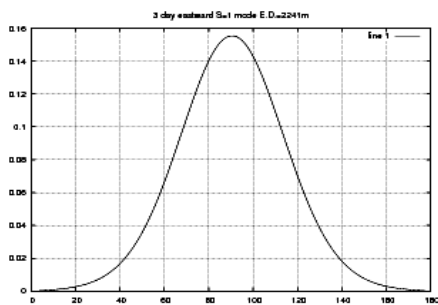


Figure 4: Hough function of eastward propagating 3 day period with $s=1$ mode. X-axis is latitude that from 0 which corresponds 90°S to 180 which corresponds 90°N . Y-axis shows the non-dimensional amplitude of the geopotential height field.

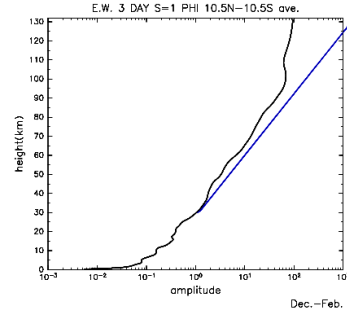


Figure 5: The vertical profile of eastward propagating 3 day period with zonal wavenumber 1 components of the geopotential height field averaged over 10.5°N to 10.5°S . Heights are from 0 km to 130 km (the black line). The Blue line is the curve of $\exp(z/2H)$.

4. Concluding Remarks

In present analysis, we have shown that eastward propagating with $s=1$ components in the period band of 2-4 days of the wind and geopotential height fields have structures of equatorial Kelvin waves (only the results of eastward propagating 3 day with $s=1$ components are shown in this proceeding). Phase lines of the zonal wind and geopotential height fields show that energy of this kind of waves propagates upward and the propagation of phase is downward while this kind of waves propagates eastward. The vertical profile of the geopotential height field shows that this kind of waves propagates vertically with nearly energy conserving in the height region between 20 km and 100km and excitation sources of this kind of wave may exist in the region lower than 20 km. The averaged vertical wavelength estimated from figure 3 is not only consistent with the theoretical solution of the Laplace's tidal equation but also consistent with observation facts indicated by Pancheva et al. (2004), and the latitudinal distribution is also consistent with numerical results and observation results shown by Forbes (2000).

5. References

- Forbes, J. M., 2000: Wave coupling between the lower and upper atmosphere: case study of an ultra-fast Kelvin Wave. *Journal of Atmospheric and Solar-Terrestrial Physics*, Vol.62, p. 1603-1621.
- Hirota, I., 1977: Equatorial Waves in the Upper Stratosphere and mesosphere in Relation to the Semiannual Oscillation of the Zonal Wind. *Journal of the Atmospheric Sciences*, Vol. 35, p. 714-722.
- Matsuno, T., 1966: Quasi-Geostrophic Motions in the Equatorial Area. *Journal of the Meteorological Society of Japan*, Vol.44, p. 25-43.
- Mayr, H. G., J.G. Mengel, E. R. Talaat, H.S. Porter, and K. L. Chan, 2004: Modeling study of mesospheric planetary waves: genesis and characteristics. *Annales Geophysicae*, Vol.22, p. 1885-1902.
- Pancheva, D., N. J. Mitchell, and P. T. Younger, 2004: Meteor radar observations of atmosphere waves in the equatorial mesosphere/lower thermosphere over Ascension Island. *Annales Geophysicae*, Vol.22, p. 387-404.
- Riggin, D. M., D. C. Fritts, T. Tsuda, T. Nakamura, and R. A. Vincent, 1997: Radar observations of a 3-day Kelvin wave in the equatorial mesosphere. *Journal of Geophysical Research*, Vol.102, No.D22, P.26, 141-26,157.
- Salby, M. L., D. L. Hartmann, and P. L. Bailey, and J. C. Gille, 1983: Evidence for Equatorial Kelvin Modes in Nimbus-7 LIMS. *Journal of the Atmospheric Sciences*, Vol.41, p. 220-235.

Yoshikawa, M. and S. Miyahara, 2005: Excitations of nonmigrating diurnal tides in the mesosphere and lower thermosphere simulated by the Kyushu-GCM. *Advances in Space Research*, Vol.35, p. 1918-1924.